A micromechanical model based on hypersingular integro-differential equations for analyzing micro-crazed interfaces between dissimilar elastic materials

Xue Wang, Whye-Teong Ang and Hui Fan
School of Mechanical and Aerospace Engineering
Nanyang Technological University, Singapore

Abstract

The current work models a weak (soft) interface between two elastic materials as containing a periodic array of micro-crazes. The boundary conditions on the interfacial micro-crazes are formulated in terms of a system of hypersingular integro-differential equations with unknown functions given by the displacement jumps across opposite faces of the micro-crazes. Once the displacement jumps are obtained by approximately solving the integro-differential equations, the effective stiffness of the micro-crazed interface can be readily computed. The effective stiffness is an important quantity needed for expressing the interfacial conditions in the spring-like macro-model of soft interfaces. Specific case studies are conducted to gain physical insights into how the effective stiffness of the interface may be influenced by the details of the interfacial micro-crazes.

Keywords: Micromechanical modeling, micro-crazed interface, effective stiffness coefficients, hypersingular integro-differential equations.

This is a pre-print of an article accepted for publication in the Springer journal *Applied Mathematics and Mechanics.* The article may be viewed at: https://doi.org/10.1007/s10483-020-2563-8

1 Introduction

At the macroscopic level, a soft imperfect interface between two dissimilar elastic materials denoted by 1 and 2 may be modeled as a continuous distribution of springs with interfacial conditions

$$\underline{\underline{\boldsymbol{\sigma}}}^{(1)} \cdot \underline{\mathbf{n}} = \underline{\underline{\boldsymbol{\sigma}}}^{(2)} \cdot \underline{\mathbf{n}} = \underline{\underline{\mathbf{k}}} \cdot (\underline{\mathbf{u}}^{(1)} - \underline{\mathbf{u}}^{(2)}) \quad \text{on } \Gamma, \tag{1}$$

where Γ denotes the interface, $\underline{\mathbf{n}}$ is the unit normal vector to Γ pointing into material 1, $\underline{\mathbf{u}}^{(i)}$ and $\underline{\underline{\boldsymbol{\sigma}}}^{(i)}$ are respectively the displacement and the stress in material i and the second rank tensor $\underline{\underline{\mathbf{k}}}$ characterizes the stiffness of the interface. Such a macro-model is well established (Benveniste and Miloh [2] and Hashin [8]) and has been widely used in analyses involving soft interfaces by many authors (see, for example, Fan and Wang [6], Jones and Whittier [10], Sudak [14] and Sudak and Wang [15]).

In recent years, Wang *et al.* [18] proposed micromechanical models for estimating the effective stiffness $\underline{\underline{\mathbf{k}}}$ of soft interfaces between elastic materials. In those models, the interfaces are assumed to be weakened by interfacial micro-cracks. It may be, however, more realistic to model soft interfaces between materials like glassy polymers as containing micro-crazes. After all, micro-crazes are precursors of micro-cracks (Gent and Thomas [7], Kuo *et al.* [12], Wang and Kramer [17], Xiao and Pae [22] and Zhang et al. [24]-[25]).

In many papers, such as Walton and Weitsman [16], Weitsman [19] and Xiao and Guo [21], opposite faces of a craze are assumed to be connected by only straight parallel fibrils. Those fibrils are modeled as a continuous distribution of parallel springs normal to the craze faces. Nevertheless, the experimental works in Brown [3] and Yang and Kramer [23] reveal the existence of cross-tie fibrils that connect the main straight parallel fibrils and are capable of bearing small lateral loads. As such, a craze is more completely modeled as a continuous distribution of anisotropic springs, as in Xiao and Curtin [20]. The fibrils at the center of a craze may break down such that

the void between the upper and lower surfaces of the broken fibrils forms a crack. After that, the crack may propagate towards the tips of the craze as more fibrils fail. Other works that examine the main fibrils and cross-tie fibrils in micro-crazes include Hui *et al.* [9] and Sha *et al.* [13].

To estimate the effective stiffness $\underline{\underline{\mathbf{k}}}$ needed in the macro-model for the soft interface, the current paper proposes a micromechanical model where the soft interface between two elastic half-spaces is regarded as microscopically damaged by a periodic array of micro-crazes. The boundary value problem of the micro-crazed interface model which we propose here is formulated in terms of hypersingular integro-differential equations. Such a formulation is advantageous in micromechanical analysis of imperfect interfaces because the displacement jumps across imperfect interfaces appear as unknown functions in the hypersingular integro-differential equations. Hence no post-processing procedure is required for calculating the interfacial displacement jumps. Once the displacement jumps are obtained by solving the integro-differential equations approximately, the effective stiffness of the interface can be readily computed. Specific case studies are conducted to gain physical insights into how the effective properties of the interface may be influenced by the details of the interfacial micro-crazes.

To the best of our knowledge, the current literature does not have any existing work on the effective behaviors of interfaces containing micro-crazes, even though there are many papers (such as those cited in the second and third paragraphs in this section) on theoretical and experimental studies of crazes in solids. The micro-mechanical (micro-craze) model proposed in the current paper for the soft interface is more realistic than the ones in Wang *et al.* [18] where the interface is modeled by interfacial micro-cracks. It contributes to a better estimation and physical understanding of the effective behaviors of soft imperfect interfaces.

2 Micro-crazed interfaces

With reference to a Cartesian coordinate system $Ox_1x_2x_3$, consider two elastic half-spaces occupying the regions $x_2 > 0$ and $x_2 < 0$. They are joined at the interface $x_2 = 0$ that is microscopically damaged by a periodic array of interfacial micro-crazes. The micro-crazes occupy the regions $a + nL < x_1 < b + nL$, $x_2 = 0$, $-\infty < x_3 < \infty$, for $n = 0, \pm 1, \pm 2, \cdots$, where a, b and L are real numbers such that $a < b$ and $L > b - a$. Refer to Figure 1.

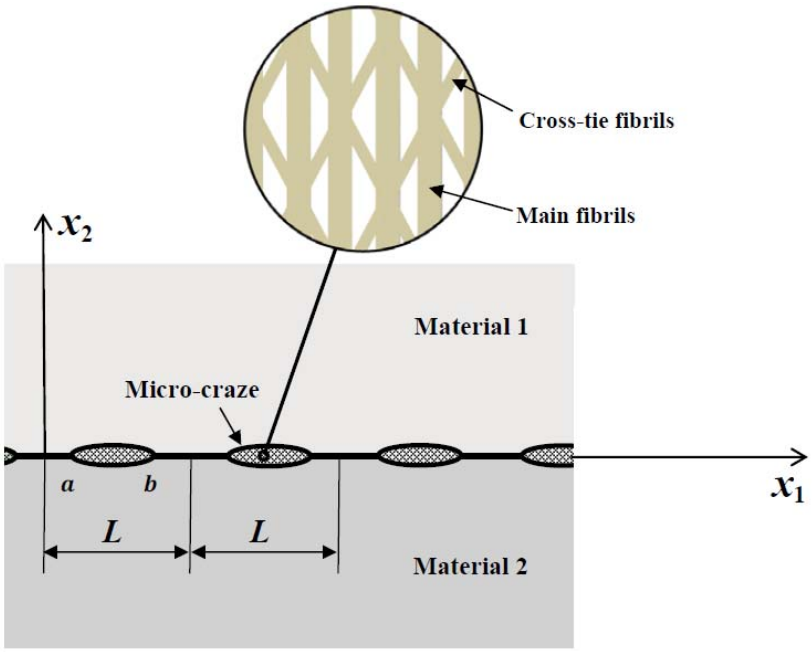

Figure 1. Periodic micro-crazes on the interface between two elastic half-spaces.

The micro-craze density ρ of the interface is defined by

$$\rho = \frac{b-a}{L}. \tag{2}$$

If the bimaterial in Figure 1 is subject to a plane elastostatic deformation such that the Cartesian displacements u_i and stresses σ_{ij} are independent of the coordinate x_3. According to the generalized Hooke's Law, the elastic stresses are given by

$$\sigma_{ij} = C_{ijkq}\frac{\partial u_k}{\partial x_q} \ (i,j=1,2), \tag{3}$$

where C_{ijkq} are the elastic moduli of the half-spaces given by

$$C_{ijkq} = \begin{cases} C^{(1)}_{ijkq} & \text{for } x_2 > 0, \\ C^{(2)}_{ijkq} & \text{for } x_2 < 0, \end{cases} \tag{4}$$

with $C^{(p)}_{ijkq}$ being positive constants such that

$$C^{(p)}_{ijkq}\xi_{ij}\xi_{kq} > 0$$

$$\text{where } \xi_{ij} \text{ are real constants such that } \sum_{i=1}^{2}\sum_{j=1}^{2}\xi_{ij}^2 \neq 0.$$

Note that all the lowercase Latin subscripts take the values 1 and 2 and follow the Einstenian convention of summing over a repeated index.

Substitution of Eq. (3) into the stress equilibrium equation of elasticity (that is, $\partial\sigma_{ij}/\partial x_j = 0$) gives rise to the elliptic system of partial differential equations

$$C_{ijkq}\frac{\partial^2 u_k}{\partial x_j \partial x_q} = 0. \tag{5}$$

For such a bimaterial, the conditions on the micro-crazed interface $x_2 = 0$ are given by (Fan and Keer [5])

$$\begin{aligned} u_i(x_1,0^+) &= u_i(x_1,0^-) \text{ for } x_1 \in U^{(n)} \ (n=0,\pm1,\pm2,\cdots), \\ \sigma_{i2}(x_1,0^+) &= \sigma_{i2}(x_1,0^-) \text{ for } x_1 \in (-\infty,\infty), \\ \sigma_{i2}(x_1,0^+) &= E_{ij}(x_1)\Delta u_j(x_1) \text{ for } x_1 \in C^{(n)} \ (n=0,\pm1,\pm2,\cdots), \end{aligned} \tag{6}$$

where $U^{(n)} = (nL, a+nL) \cup (b+nL, (n+1)L)$ and $C^{(n)} = (a+nL, b+nL)$ are the intervals on the perfect and the micro-crazed parts of the interface

respectively, $E_{ij}(x_1)$ are the micro-craze stiffness coefficients given by periodic functions of x_1 with period L, $\Delta u_j(x_1) = u_j(x_1, 0^+) - u_j(x_1, 0^-)$ are the displacement jumps across opposite faces of the micro-crazes. Note that $E_{ij} = 0$ gives the special case of micro-cracks occupying the interface between the two half-spaces.

The displacements u_i and stresses σ_{i2} may be homogenized over a macroscopic portion of the interface of length 2δ by the averaging procedure

$$\begin{aligned} \overline{u}_i(\overline{x}_1, 0^{\pm}) &= \frac{1}{2\delta} \int_{\overline{x}_1 - \delta}^{\overline{x}_1 + \delta} u_i(x_1, 0) dx_1, \\ \overline{\sigma}_{i2}(\overline{x}_1, 0^{\pm}) &= \frac{1}{2\delta} \int_{\overline{x}_1 - \delta}^{\overline{x}_1 + \delta} \sigma_{i2}(x_1, 0) dx_1, \end{aligned} \tag{7}$$

where $\overline{x}_1$ denotes the center of the macroscopic portion of the interface.

The macro-model for the soft imperfect interface in (1) can be rewritten in terms of the homogenized interfacial displacements and stresses as

$$\overline{\sigma}_{i2}(\overline{x}_1, 0^+) = \overline{\sigma}_{i2}(\overline{x}_1, 0^-) = k_{ij}(\overline{u}_j(\overline{x}_1, 0^+) - \overline{u}_j(\overline{x}_1, 0^-)), \tag{8}$$

where k_{ij} are the Cartesian components of the interface stiffness $\underline{\underline{\mathbf{k}}}$.

The stiffness components k_{ij} in the macro-model of the soft imperfect interface may be estimated by calculating the effective stiffness of the micro-crazed interface described above. The problem of interest here is to examine how the details of the interfacial micro-crazes, such as the micro-craze density ρ and the micro-craze stiffness E_{ij} in (6), influence the interface stiffness k_{ij}.

3 Boundary value problem

Let the elastic displacements u_i and the stresses σ_{ij} in the bimaterial with the micro-crazed interface in Section 2 be given by

$$\begin{aligned} u_i &= u_i^{(\mathrm{per})} + u_i^{(\mathrm{cr})}, \\ \sigma_{ij} &= \sigma_{ij}^{(\mathrm{per})} + \sigma_{ij}^{(\mathrm{cr})}, \end{aligned} \tag{9}$$

where $u_i^{(\mathrm{per})}$ and $\sigma_{ij}^{(\mathrm{per})}$ are respectively the displacements and the stresses in the bimaterial for the case where the interface between the elastic half-spaces is wholly perfect and $u_i^{(\mathrm{cr})}$ and $\sigma_{ij}^{(\mathrm{cr})}$ are respectively the perturbing displacements and stresses caused by the interfacial micro-crazes.

Thus, the interfacial conditions in (6) may be rewritten as

$$\begin{aligned} \Delta u_i^{(\mathrm{cr})}(x_1) &= 0 \text{ for } x_1 \in U^{(n)} \ (n = 0, \pm 1, \pm 2, \cdots), \\ \sigma_{i2}^{(\mathrm{cr})}(x_1, 0^+) &= \sigma_{i2}^{(\mathrm{cr})}(x_1, 0^-) \text{ for } x_1 \in (-\infty, \infty), \\ \sigma_{i2}^{(\mathrm{cr})}(x_1, 0^\pm) &= -\sigma_{i2}^{(\mathrm{per})}(x_1, 0^+) + E_{ij}(x_1)\Delta u_j^{(\mathrm{cr})}(x_1) \\ \text{for } x_1 &\in C^{(n)} \ (n = 0, \pm 1, \pm 2, \cdots). \end{aligned} \tag{10}$$

As described in Section 2, the micro-crazes are considered as periodically repeated along the entire interface, the $u_i^{(\mathrm{per})}$ and $\sigma_{ij}^{(\mathrm{per})}$ are therefore assumed to be periodic functions of x_1 with periodic L (such as the case where $u_i^{(\mathrm{per})}$ and $\sigma_{ij}^{(\mathrm{per})}$ are linear functions of x_2 only and constant functions respectively). With the periodic loads $\sigma_{ij}^{(\mathrm{per})}$ acting on the interfacial micro-crazes, u_i and σ_{ij} are also periodic functions of x_1 with periodic L.

The boundary value problem here is to solve the governing equations in (5) for $u_i^{(\mathrm{cr})}$ together with (4) subject to the interfacial conditions in (10) and the far field conditions $\sigma_{rj}^{(\mathrm{cr})} \to 0$ as $|x_2| \to \infty$.

4 Hypersingular integro-differential equations

To solve the boundary value problem, suitable Fourier integral representations are used in this section to derive the hypersingular integro-differential equations for the interfacial micro-crazes. The analysis in Ang [1] is followed closely here. Note that the derivations in [1] are for micro-cracks, that is, for the case where $E_{jr} = 0$.

For the bimaterial, the displacements $u_r^{(\mathrm{cr})}$ are written as the general

solutions for the partial differential equations (5) given by

$$u_r^{(\mathrm{cr})}(\xi_1,\xi_2)=\begin{cases}\mathrm{Re}\{\sum\limits_{\alpha=1}^{2}A_{r\alpha}^{(1)}f_\alpha(\xi_1+\tau_\alpha^{(1)}\xi_2)\} & \text{for } \xi_2>0,\\ \mathrm{Re}\{\sum\limits_{\alpha=1}^{2}A_{r\alpha}^{(2)}g_\alpha(\xi_1+\tau_\alpha^{(2)}\xi_2)\} & \text{for } \xi_2<0,\end{cases} \tag{11}$$

where Re denotes the real part of a complex number, the complex functions f_α and g_α are taken to be in the Fourier integral form:

$$\begin{aligned} f_\alpha(\xi_1+\tau_\alpha^{(1)}\xi_2) &= \int_0^\infty E_\alpha^{(1)}(\zeta)\exp(i\zeta[\xi_1+\tau_\alpha^{(1)}\xi_2])d\zeta,\\ g_\alpha(\xi_1+\tau_\alpha^{(2)}\xi_2) &= \int_0^\infty E_\alpha^{(2)}(\zeta)\exp(-i\zeta[\xi_1+\tau_\alpha^{(2)}\xi_2])d\zeta, \end{aligned} \tag{12}$$

with $E_\alpha^{(1)}(\zeta)$ and $E_\alpha^{(2)}(\zeta)$ being complex functions yet to be determined, $\tau_1^{(p)}$ and $\tau_2^{(p)}$ are complex numbers with positive imaginary parts and satisfy the quartic equation given by

$$\begin{aligned} \det[C_{i1k1}^{(p)}+(C_{i1k2}^{(p)}+C_{i2k1}^{(p)})\tau_\alpha^{(p)}+C_{i2k2}^{(p)}(\tau_\alpha^{(p)})^2] &= 0\\ \text{for } p &= 1,2, \end{aligned}$$

and $[A_{r\alpha}^{(p)}]$ are non-null 2×2 matrix satisfying

$$[C_{i1k1}^{(p)}+(C_{i1k2}^{(p)}+C_{i2k1}^{(p)})\tau_\alpha^{(p)}+C_{i2k2}^{(p)}(\tau_\alpha^{(p)})^2]A_{k\alpha}^{(p)}=0.$$

One may verify by direct substitution that the displacements $u_r^{(\mathrm{cr})}(\xi_1,\xi_2)$ given by (11) together with (12) satisfy the partial differential equations in (5). For details on the derivation of (11) and (12) and the approach used here to solve the boundary value problem, one may refer to Clements [4]. As shown below, the task of determining the unknown functions $E_\alpha^{(1)}(\zeta)$ and $E_\alpha^{(2)}(\zeta)$ in (12) in order to satisfy the interfacial conditions in (10) leads to hypersingular integro-differential equations with the displacement jumps across opposite micro-craze faces as unknown functions.

Substitution of (11) into (3) gives rise to the stress formulae

$$\sigma_{rj}^{(\mathrm{cr})}(\xi_1,\xi_2)=\begin{cases}\mathrm{Re}\{\sum\limits_{\alpha=1}^{2}L_{rj\alpha}^{(1)}f_\alpha'(\xi_1+\tau_\alpha^{(1)}\xi_2)\} & \text{for } \xi_2>0,\\ \mathrm{Re}\{\sum\limits_{\alpha=1}^{2}L_{rj\alpha}^{(2)}g_\alpha'(\xi_1+\tau_\alpha^{(2)}\xi_2)\} & \text{for } \xi_2<0,\end{cases} \tag{13}$$

where $L_{rj\alpha}^{(p)}$ are constants given by

$$L_{rj\alpha}^{(p)}=(C_{rjk1}^{(p)}+\tau_\alpha^{(p)}C_{rjk2}^{(p)})A_{k\alpha}^{(p)}.$$

Note that the usual Einstenian convention of summing a repeated index is assumed for only Latin subscripts.

To ensure that the stresses σ_{r2} are continuous on the entire interface $x_2=0$, we take

$$\begin{aligned}E_\alpha^{(1)}(\zeta) &= M_{\alpha q}^{(1)}\phi_q(\zeta),\\ E_\alpha^{(2)}(\zeta) &= M_{\alpha q}^{(2)}\overline{\phi}_q(\zeta),\end{aligned} \tag{14}$$

where $[M_{\alpha q}^{(p)}]$ is the inverse of $[L_{\alpha 2q}^{(p)}]$ and $\phi_q(\zeta)$ are functions yet to be determined.

If $\phi_q(\zeta)$ is chosen to be

$$\phi_q(\zeta)=iQ_{qj}\sum_{n=-\infty}^{\infty}\int_{a+nL}^{b+nL}r_j(x_1)\exp(-i\zeta x_1)dx_1, \tag{15}$$

where Q_{qj} are complex constants and $r_j(x_1)$ are real functions, then

$$\begin{aligned}&u_r(\xi_1,0^+)-u_r(\xi_1,0^-)\\ =\;&-\lim_{\varepsilon\to 0^+}\sum_{n=-\infty}^{\infty}\int_{a+nL}^{b+nL}r_j(x_1)\,\mathrm{Re}\{\sum_{\alpha=1}^{2}Q_{qj}[\frac{A_{r\alpha}^{(1)}M_{\alpha q}^{(1)}}{\xi_1-x_1+\tau_\alpha^{(1)}\varepsilon}\\ &-\frac{\overline{A}_{r\alpha}^{(2)}\overline{M}_{\alpha q}^{(2)}}{\xi_1-x_1-\overline{\tau}_\alpha^{(2)}\varepsilon}]\}dx_1.\end{aligned} \tag{16}$$

If the constants Q_{qj} are implicitly defined by

$$\pi Q_{jr} \sum_{\alpha=1}^{2} [A_{k\alpha}^{(1)} M_{\alpha j}^{(1)} - \overline{A}_{k\alpha}^{(2)} \overline{M}_{\alpha j}^{(2)}] = -i\delta_{kr}, \tag{17}$$

we can show that (16) satisfies $u_i(\xi_1, 0^+) - u_i(\xi_1, 0^-) = 0$ on the perfectly bonded areas of the interface and $r_i(x_1)$ is equal to the displacement jumps $\Delta u_i^{(\mathrm{cr})}(x_1)$ across the micro-crazes (see [1]).

From (12)–(15) and the summation formula

$$\sum_{n=1}^{\infty} \frac{1}{(z_1 \pm n z_2)^2} = \frac{1}{z_2^2} \Psi_1(1 \pm \frac{z_1}{z_2})$$
$$\text{for } |z_2| \neq 0 \text{ and } \mathrm{Re}\{1 \pm \frac{z_1}{z_2}\} > 0, \tag{18}$$

where z_1 and z_2 are complex constants and $\Psi_1(z)$ is the trigamma function, the interfacial conditions in (10) for the micro-crazes may be written into the hypersingular integro-differential equations

$$\begin{aligned} & \oint_a^b \frac{\mathrm{Re}\{Q_{jr}\} \Delta u_r^{(\mathrm{cr})}(x_1)}{(x_1 - \xi_1)^2} dx_1 \\ & + \int_a^b \mathrm{Re}\{Q_{jr}\} \Delta u_r^{(\mathrm{cr})}(x_1) \Theta(x_1, \xi_1) dx_1 - \mathrm{Im}\{\pi Q_{jr}\} \frac{d}{d\xi_1} (\Delta u_r^{(\mathrm{cr})}(\xi_1)) \\ = \; & -\sigma_{j2}^{(\mathrm{per})}(\xi_1, 0) + E_{jr}(\xi_1) \Delta u_r^{(\mathrm{cr})}(\xi_1) \text{ for } a < \xi_1 < b, \end{aligned} \tag{19}$$

where $\oint$ denotes that the integral is to be interpreted in the Hadamard finite-part sense, Im denotes the imaginary part of a complex number and the function $\Theta(x_1, \xi_1)$ is defined by

$$\Theta(x_1, \xi_1) = \frac{1}{L^2} \Psi_1(\frac{L + x_1 - \xi_1}{L}) + \frac{1}{L^2} \Psi_1(\frac{L + \xi_1 - x_1}{L}). \tag{20}$$

Note that the constants Q_{jr} depend on the elastic moduli of the material half-spaces and the hypersingular integro-differential equations in (19) are essentially those given in Ang [1] for the special case where $E_{jr} = 0$ (that is, for interfacial cracks).

To compute the effective stiffness of the micro-crazed interface, as given by k_{ij} in (8), the hypersingular integro-differential equations in (19) are solved for the displacement jumps across opposite faces of the micro-crazes by using $\sigma_{j2}^{(\mathrm{per})}(x_1,0) = P_j^{(A)}$ and $\sigma_{j2}^{(\mathrm{per})}(x_1,0) = P_j^{(B)}$, where $P_j^{(A)}$ and $P_j^{(B)}$ are constants such that $P_j^{(A)}$ and $P_j^{(B)}$ are linearly independent vectors (that is, $P_j^{(A)}$ and $P_j^{(B)}$ are not scalar multiples of each other). If the displacement jumps obtained by using the loads $\sigma_{j2}^{(\mathrm{per})}(x_1,0) = P_j^{(A)}$ and $\sigma_{j2}^{(\mathrm{per})}(x_1,0) = P_j^{(B)}$ are respectively denoted by $\Delta u_r^{(A)}(x_1)$ and $\Delta u_r^{(B)}(x_1)$, the effective stiffness k_{ij} may be obtained by solving the system

$$\left.\begin{array}{l} \dfrac{k_{jr}}{L}\displaystyle\int_a^b \Delta u_r^{(A)}(x_1)dx_1 = P_j^{(A)} \\ \dfrac{k_{jr}}{L}\displaystyle\int_a^b \Delta u_r^{(B)}(x_1)dx_1 = P_j^{(B)} \end{array}\right\} \text{ for } j = 1, 2. \tag{21}$$

5 Numerical procedures

The numerical procedures for solving the hypersingular integro-differential equations (19) are outlined below.

The collocation technique in Kaya and Erdogan [11] is used here to solve (19) approximately. The unknown displacement jumps $\Delta u_r^{(\mathrm{cr})}(x_1)$ are written in the form

$$\begin{aligned} \Delta u_r^{(\mathrm{cr})}(x_1) \;\simeq\; & \sqrt{(x_1-a)(b-x_1)} \\ & \times \sum_{m=1}^{N_\mathrm{c}} \alpha_r^{(m)} U^{(m-1)}\Big(\frac{2x_1-b-a}{b-a}\Big) \\ & \text{for } a < x_1 < b, \end{aligned} \tag{22}$$

where N_c is a positive integer which may be required to be sufficiently large for (22) to be a good approximation, $\alpha_r^{(1)}, a_r^{(2)}, \cdots, \alpha_r^{(N_\mathrm{c}-1)}$ and $\alpha_r^{(N_\mathrm{c})}$ are constant coefficients to be determined and $U^{(m)}(x)$ is the m-th order Chebyshev polynomials of the second kind.

Substituting (22) into (19) and collocating the resulted equations at $N_{\rm c}$ points (over the micro-craze) given by

$$(\widetilde{x}_{\rm c}^{(m)}, 0) = (\frac{b+a}{2} + \frac{b-a}{2}\cos(\frac{[2m-1]\pi}{2N_{\rm c}}), 0) \quad \text{for } m = 1, 2, \cdots, N_{\rm c}, \tag{23}$$

reduce the hypersingular integro-differential equations to the linear algebraic equations

$$\begin{aligned}
&-\sum_{m=1}^{N_{\rm c}} \alpha_r^{(m)} \,{\rm Re}\{Q_{jr}\}\pi m U^{(m-1)}(\frac{2\widetilde{x}_{\rm c}^{(n)} - b - a}{b-a}) \\
&-\sum_{m=1}^{N_{\rm c}} \alpha_r^{(m)} E_{jr}(\widetilde{x}_{\rm c}^{(n)})\ \sqrt{(\widetilde{x}_{\rm c}^{(n)} - a)(b - \widetilde{x}_{\rm c}^{(n)})}\, U^{(m-1)}(\frac{2\widetilde{x}_{\rm c}^{(n)} - b - a}{b-a}) \\
&+\sum_{m=1}^{N_{\rm c}} \alpha_r^{(m)} \,{\rm Re}\{Q_{jr}\} \int_a^b \sqrt{(x_1 - a)(b - x_1)} \\
&\times U^{(m-1)}(\frac{2x_1 - b - a}{b-a})\Theta(x_1, \widetilde{x}_{\rm c}^{(n)})dx_1 \\
&-\sum_{m=1}^{N_{\rm c}} \alpha_r^{(m)} \,{\rm Im}\{\pi Q_{jr}\} \frac{(a-b)m\cos[m\arccos(\frac{2\widetilde{x}_{\rm c}^{(n)} - b - a}{b-a})]}{2\sqrt{(\widetilde{x}_{\rm c}^{(n)} - a)(b - \widetilde{x}_{\rm c}^{(n)})}} \\
= &- P_j \\
\text{for } n = &\ 1, 2, ..., N_{\rm c}.
\end{aligned} \tag{24}$$

Once the linear algebraic equations (24) are solved using the two independent loads $[P_1^{(A)}, P_2^{(A)}]$ and $[P_1^{(B)}, P_2^{(B)}]$, the effective stiffness coefficients k_{ij} may be calculated from (21) by simultaneously

$$\begin{aligned}
&k_{ij} \sum_{m=1}^{N_{\rm c}} \alpha_j^{(\ell m)} \int_a^b \sqrt{(x_1 - a)(b - x_1)} \\
&\times U^{(m-1)}(\frac{2x_1 - b - a}{b-a})dx_1 = P_i^{(\ell)} L \\
&\qquad\qquad \text{for } \ell = A, B.
\end{aligned} \tag{25}$$

Note that $\alpha_j^{(\ell m)}$ are the constants $\alpha_j^{(m)}$ in (24) for $P_j = P_j^{(\ell)}$ with $\ell = A, B$.

For the problems in the specific case studies below, we have calculated k_{ij} using many different sets of linearly independent loads $[P_1^{(A)}, P_2^{(A)}]$ and $[P_1^{(B)}, P_2^{(B)}]$. For a particular problem, the different sets of loads give the same value of k_{ij} if there is no change in the other parameters that define the problem.

6 Specific case studies

For particular case studies, we take materials 1 and 2 in the half-spaces to be isotropic polymers. The elastic moduli $C_{ijkq}^{(n)}$ of material n are given by

$$C_{ijkq}^{(n)} = \begin{cases} \lambda^{(n)} + 2\mu^{(n)} & \text{if } (i,j,k,q) = (1,1,1,1), \\ \lambda^{(n)} & \text{if } (i,j,k,q) = (1,1,2,2) = (2,2,1,1), \\ \lambda^{(n)} + 2\mu^{(n)} & \text{if } (i,j,k,q) = (2,2,2,2), \\ \mu^{(n)} & \text{if } (i,j,k,q) = (1,2,1,2) = (2,1,2,1) \\ & \qquad = (1,2,2,1) = (2,1,1,2), \\ 0 & \text{otherwise,} \end{cases} \tag{26}$$

where $\lambda^{(n)}$ and $\mu^{(n)}$ are the Lamé constants of the isotropic materials.

The materials in the half-spaces may be isotropic or anisotropic. We choose isotropic materials for our case studies because most of the existing works in the literature deal with crazes in isotropic materials such as glass polymers which are widely used in engineering applications. Another reason for choosing isotropic materials is to show below how the general analysis in the paper can be used to recover the special case where the half-spaces are occupied by isotropic materials.

The constants $M_{\alpha q}^{(n)}$ in (14) is ill-defined for the elastic moduli $C_{ijkq}^{(n)}$ in (26). Nevertheless, if we proceed as in [1] by replacing $C_{1122}^{(p)} = C_{2211}^{(p)} = \lambda^{(p)}$ in (26) with $C_{1122}^{(p)} = C_{2211}^{(p)} = \lambda^{(p)}(1-\varepsilon)$ and letting ε tend to zero, we can reduce the hypersingular integro-differential equations in (19) for the

isotropic bimaterial to

$$\begin{aligned}
&\frac{1}{2\pi}[\not\int_a^b \frac{\Delta u_r(x_1)J_{jr}}{(x_1-\xi_1)^2}dx_1 \\
&+\int_a^b \Delta u_r(x_1)J_{jr}\Theta(x_1,\xi_1)dx_1 - \pi K_{jr}\frac{d}{d\xi_1}(\Delta u_r(\xi_1))] \\
= \;& \sigma_{j2}^{(\mathrm{per})}(x_1,0) - E_{jr}(\xi_1)\Delta u_r(\xi_1) \text{ for } a<\xi_1<b, \qquad (27)
\end{aligned}$$

where J_{ri} and K_{ri} are the real constants given by

$$\begin{aligned}
J_{jr} &= \begin{cases} \eta[(\mu_2+\mu_1)(2\mu_1\mu_2+\lambda_1\lambda_2+2\lambda_1\mu_2+2\mu_1\lambda_2) & \text{if} \quad j=r, \\ \quad -\lambda_1\mu_2^2-\lambda_2\mu_1^2] & \\ 0 & \text{if} \quad j\neq r, \end{cases} \\
K_{jr} &= \begin{cases} \eta\mu_1\mu_2(\lambda_1-\lambda_2+\mu_1-\mu_2) & \text{if} \quad j=1 \text{ and } r=2, \\ -\eta\mu_1\mu_2(\lambda_1-\lambda_2+\mu_1-\mu_2) & \text{if} \quad j=2 \text{ and } r=1, \\ 0 & \text{if} \quad j\neq r, \end{cases} \qquad (28)
\end{aligned}$$

with η defined by

$$\eta = -\frac{4\mu_1\mu_2}{(\lambda_2\mu_2+\mu_2^2+\mu_1\lambda_2+3\mu_1\mu_2)(\mu_1^2+\lambda_1\mu_1+3\mu_1\mu_2+\lambda_1\mu_2)}. \qquad (29)$$

In the results for the case studies reported below, we take the isotropic polymer in the half-space $x_2>0$ to be Polycaprolactam with Young's modulus and Poisson's ratio given by $E^{(1)}=4.00$ GPa and $v^{(1)}=0.40$ respectively, while the isotropic polymer in the half-space $x_2<0$ is taken to be Polystyrene with Young's modulus and Poisson's ratio given by $E^{(2)}=3.76$ GPa and $v^{(2)}=0.35$ respectively. Note that the Lamé constants $\lambda^{(n)}$ and $\mu^{(n)}$ are related to $E^{(n)}$ and $\nu^{(n)}$ by $\lambda^{(n)}=\nu^{(n)}E^{(n)}/((1+\nu^{(n)})(1-2\nu^{(n)}))$ and $\mu^{(n)}=E^{(n)}/(2(1+\nu^{(n)}))$.

6.1 Micro-crazes with straight parallel fibrils only and uniform stiffness

We assume that opposite faces of the micro-crazes are connected by only straight parallel fibrils, that is, the micro-crazes are modeled as continuous

distributions of springs that are parallel to the x_2 axis. For such micro-crazes, the only non-zero component of the micro-craze stiffness E_{ij} is E_{22}. Here we take $E_{ij} = \delta_{i2}\delta_{j2}E_0$, where E_0 is a given positive constant, that is, the micro-crazes have uniform stiffness. Note that the SI unit of E_0 is N/m as E_0 is the stiffness of a surface (micro-craze).

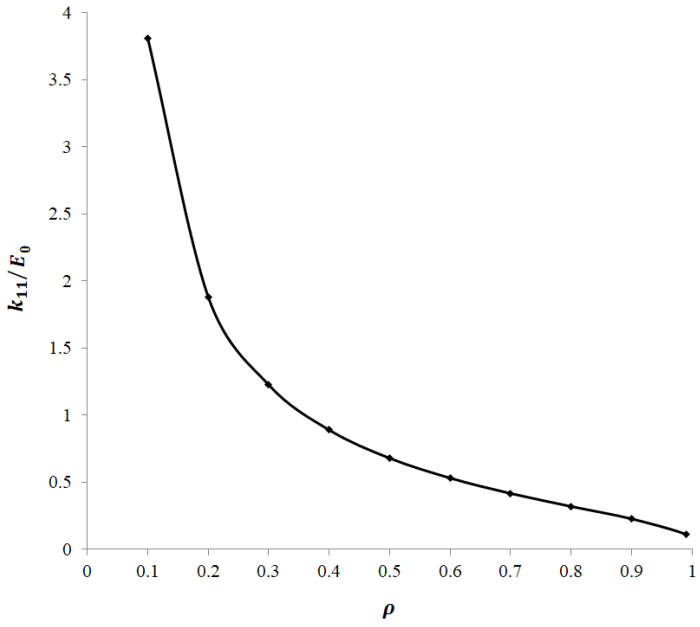

Figure 2. Plot of k_{11}/E_0 against ρ for $E_{22}/E_0 = 1$.

For $E_{22}/E_0 = 1$, we plot the non-dimensionalized stiffness coefficients k_{11}/E_0 and k_{22}/E_0 against the micro-craze density ρ in Figures 2 and 3 respectively. (We do not plot k_{12} and k_{21} here as they are found to have values with magnitudes in the order of 10^{-16} which are insignificant compared to k_{11} and k_{22}.) From the figures, we observe that k_{11}/E_0 and k_{22}/E_0 decrease as ρ increases. Such an observation is consistent with the fact that the interface is stiffer if it is micro-crazed to a lesser extent. Also, as one may expect, we find that the values of k_{11}/E_0 and k_{22}/E_0 become closer to those of E_{11}/E_0

and E_{22}/E_0 (that is, 0 and 1) respectively as ρ tends to one.

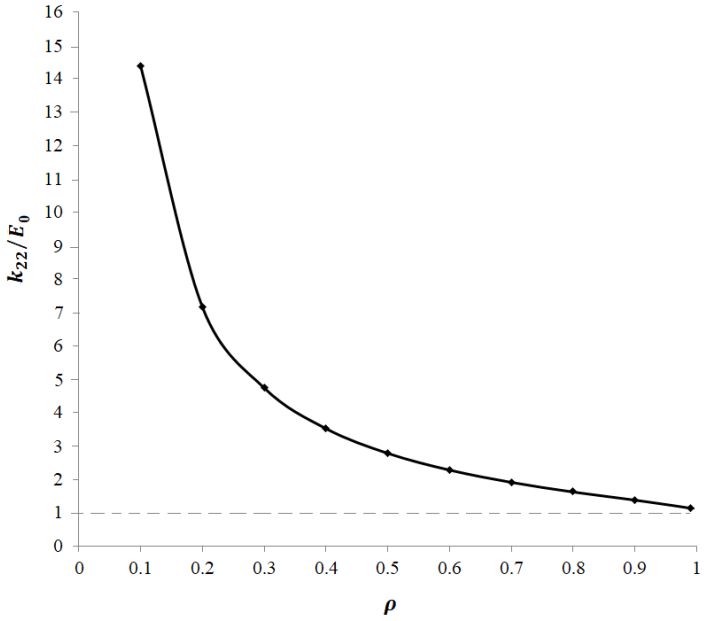

Figure 3. Plot of k_{22}/E_0 against ρ for $E_{22}/E_0 = 1$.

To examine the effects of the micro-craze stiffness on the effective stiffness of the interface, we plot k_{11}/E_0 and k_{22}/E_0 against E_{22}/E_0 for $0 \leq E_{22}/E_0 \leq 10$ and selected values of the micro-craze density ρ in Figures 4 and 5 respectively. From Figure 4, it appears that the stiffness of the straight fibrils connecting opposite faces of the micro-crazes has negligible effect on the effective stiffness k_{11} of the micro-crazed interface. As expected, for a fixed ρ, k_{22}/E_0 increases as E_{22}/E_0 increases, that is, the macro-level interface stiffness in the x_2 direction is larger if the straight fibrils which are parallel to the x_2 axis are stronger. Note that k_{22} increases almost linearly with E_{22}. We have also checked that k_{11}/E_0 and k_{22}/E_0 in Figures 4 and 5 tend to the corresponding values for the micro-cracked interface as computed by using the analysis in Wang *et al.* [18], if we let E_{22}/E_0 tend to zero.

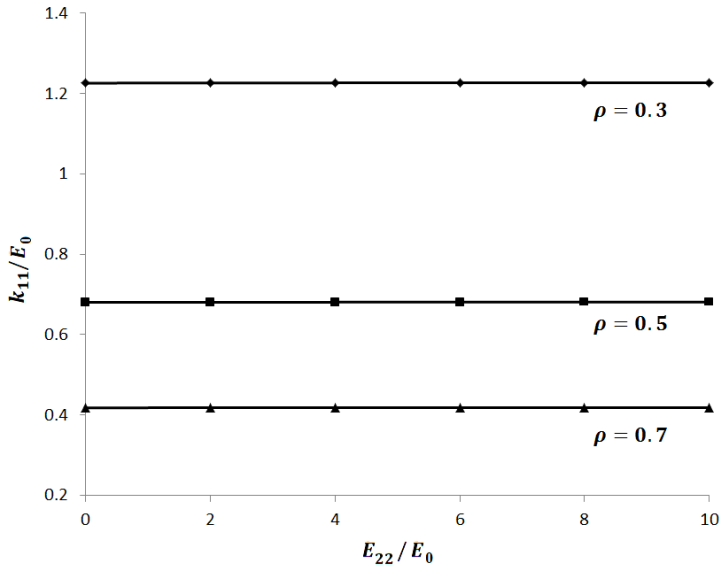

Figure 4. Plots of k_{11}/E_0 against E_{22}/E_0 for selected values of ρ.

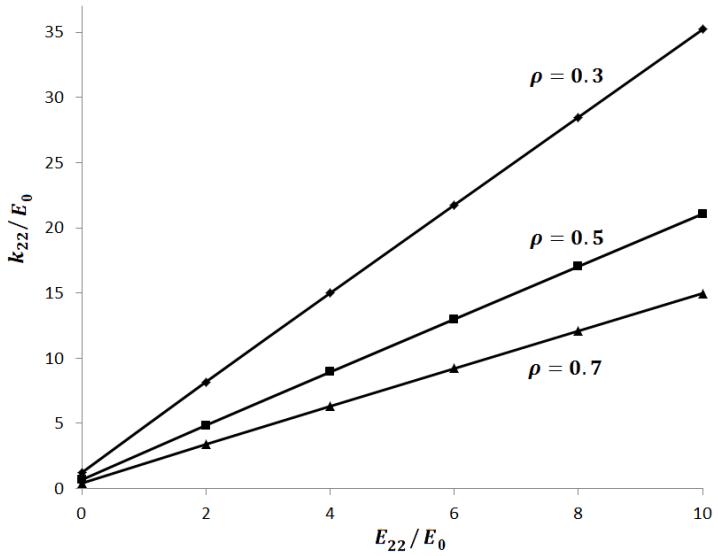

Figure 5. Plots of k_{22}/E_0 against E_{22}/E_0 for selected values of ρ.

6.2 Micro-crazes with straight parallel fibrils only and spatially varying stiffness

As before, the micro-crazes have only straight parallel fibrils connecting opposite faces, but here the only non-zero component of the micro-craze stiffness, that is E_{22}, varies continuously from point to point. Specifically, as in Walton and Weitsman [16] and Xiao and Guo [21], we take

$$\frac{E_{22}(x_1)}{E_0} = \omega\sqrt{1-(\frac{2x_1-(a+b)}{b-a})^2}+\frac{1-\omega}{\sqrt{1-(\frac{2x_1-(a+b)}{b-a})^2}} \quad \text{for } a<x_1<b, \tag{30}$$

where E_0 is a positive constant and ω is a dimensionless parameter such that $0 \leq \omega \leq 1$. If ω is a number close to 0.5, the function $E_{22}(x_1)$ in (30) is almost a constant (approximately equal to E_0) over the middle portion of the interval $a < x_1 < b$, but it gradually becomes larger and eventually tends to ∞ as x_1 approaches the micro-craze tips at $x_1 = a$ and $x_1 = b$.

As we have seen earlier on, the effect that varying E_{22} in micro-crazes connected by only straight fibrils has on k_{11} is negligible. (We have checked that k_{11} changes negligibly as ω increases from 0 to 1.) Thus, we examine here only how k_{22}/E_0 is affected by varying ω in (30). In Figure 6, we plot k_{22}/E_0 against ω for selected values of ρ. From the plots, it is obvious that k_{22}/E_0 decreases as ω increases. This observation may be physically explained as follows. The non-dimensionalized micro-craze stiffness $E_{22}(x_1)/E_0$ decreases as ω increases for $x_1 \in (a, b)$, since the partial derivative of the right hand side of (30) with respect to ω is less than zero for $x_1 \in (a, b)$. Hence, as ω increases, the micro-crazes become weaker, giving rise to a micro-crazed interface of lower effective stiffness.

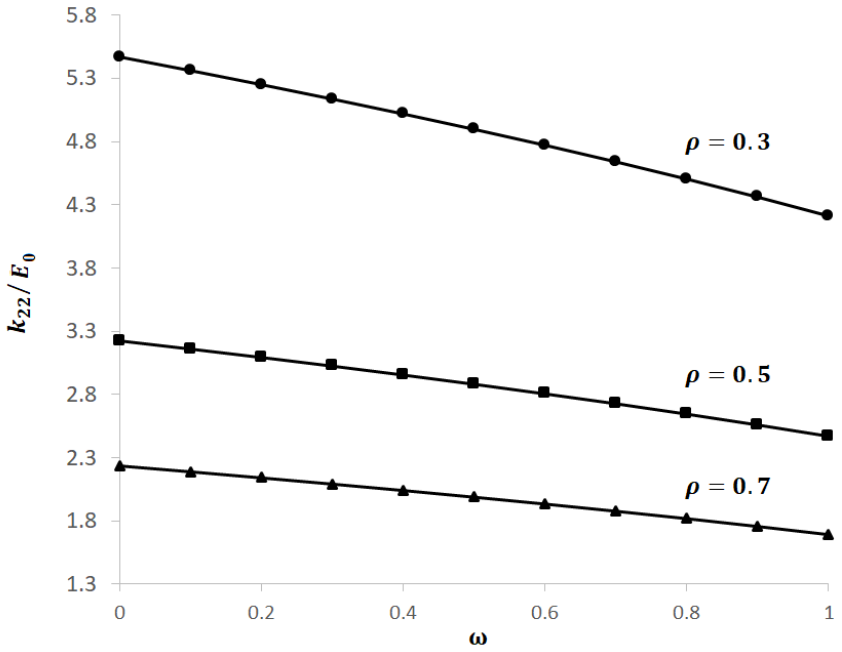

Figure 6. Plots of k_{22}/E_0 against ω for selected values of ρ.

6.3 Partially cracked micro-crazes with straight parallel fibrils only

We consider here the case in which straight parallel fibrils at the center of each of the periodic micro-crazes are broken down to form a micro-crack. Specifically, the micro-crazed stiffness E_{ij} are given over the interval $a < x_1 < b$ by $E_{12} = E_{21} = 0$ and

$$E_{22}(x_1) = \begin{cases} E_0 \quad \text{if} \quad x_1 \in (a, \dfrac{a+b}{2} - c) \cup (\dfrac{a+b}{2} + c, b), \\ \\ 0 \quad \text{if} \quad x_1 \in (\dfrac{a+b}{2} - c, \dfrac{a+b}{2} + c), \end{cases} \tag{31}$$

where E_0 is a given positive constant and c is a constant such that $0 \leq 2c \leq b - a$, that is, the micro-crack on the micro-craze $a < x_1 < b$, $x_2 = 0$ is

centrally located on the micro-craze and is of length $2c$. Note that $E_{ij} = 0$ over the cracked parts of the micro-crazes.

In Figure 7, we plot k_{22}/E_0 against $2c/(b-a)$ for selected values of ρ. From the plots, we observe that k_{22}/E_0 decreases as $2c/(b-a)$ increases. This may be explained as follows. The macro-crazes are cracked to a larger extent if the density of the cracks over the micro-crazes, that is, $2c/(b-a)$, has a larger value. Thus, as $2c/(b-a)$ increases, the micro-crazed interface becomes weaker and has lower effective stiffness. Again, as expected, the effective stiffness coefficients of the interface tend to the corresponding stiffness values (calculated using the analysis in [18]) of the fully micro-cracked interface, as $2c/(b-a)$ is approaching to 1.

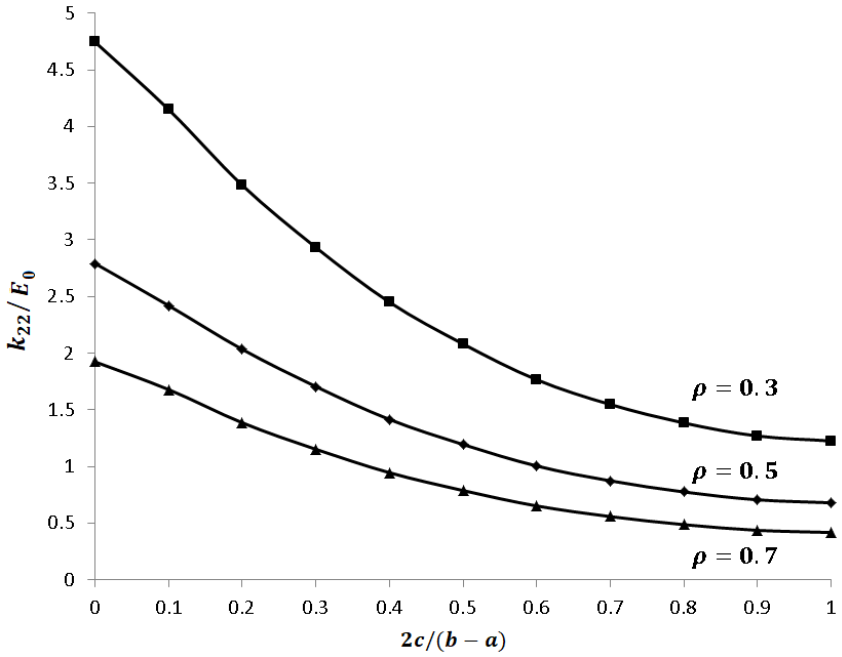

Figure 7. Plots of k_{22}/E_0 against $2c/(b-a)$ for selected values of ρ.

6.4 Micro-crazes with both straight parallel fibrils and cross-tie fibrils

The micro-craze stiffness E_{ij} are assumed to be constants. Unlike the cases above, E_{11}, E_{12} and E_{21} are not necessarily zero. Taking $E_{22}/E_0 = 1$ (where E_0 is a given constant), we are interested in examining the influences of E_{11}/E_0 and $E_{12}/E_0 = E_{21}/E_0$ on the effective stiffness of the micro-crazed interface.

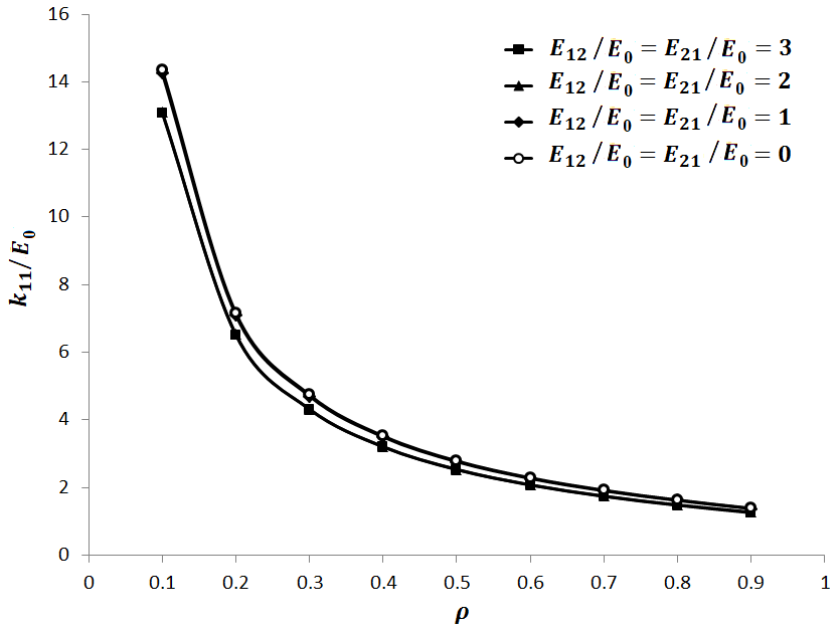

Figure 8. Plots of k_{11}/E_0 against ρ for $E_{11}/E_0 = E_{22}/E_0 = 1$ and $E_{12}/E_0 = E_{21}/E_0 = 0$, 1, 2 and 3.

For $E_{11}/E_0 = E_{22}/E_0 = 1$ and $E_{12}/E_0 = E_{21}/E_0 = 0$, 1, 2 and 3, we plot k_{11}/E_0 and k_{12}/E_0 against ρ in Figures 8 and 9 respectively. Plots of k_{22}/E_0 and k_{21}/E_0 are not presented here, as we find that the values of k_{22} and k_{21} are not significantly different from those of k_{11} and k_{12} respectively.

The plots of k_{11}/E_0 in Figure 8 for the different values of E_{12}/E_0 are very close to one another, while the corresponding plots of k_{12}/E_0 in Figure 9 are farther apart. Thus, it seems that varying the micro-crazed stiffness E_{12}/E_0 has a much larger influence on k_{12}/E_0 than k_{11}/E_0. The trends of k_{11}/E_0 and k_{12}/E_0 against ρ are the same as those in Figures 2 and 3, that is, the effective stiffness of the micro-crazed interface decreases as ρ increases. For a fixed value of ρ, k_{12}/E_0 has a higher value if E_{12}/E_0 is larger.

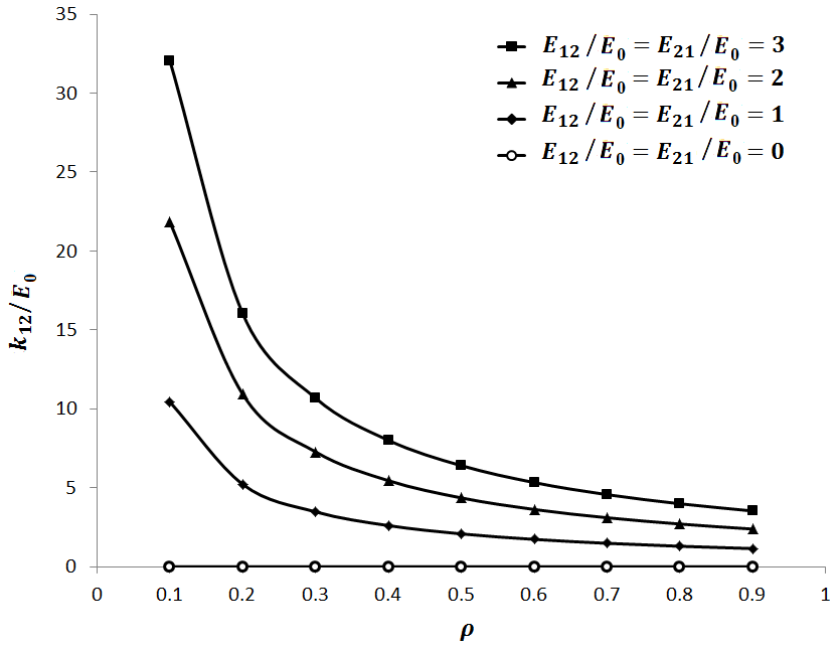

Figure 9. Plots of k_{12}/E_0 against ρ for $E_{11}/E_0 = E_{22}/E_0 = 1$ and $E_{12}/E_0 = E_{21}/E_0 = 0$, 1, 2 and 3.

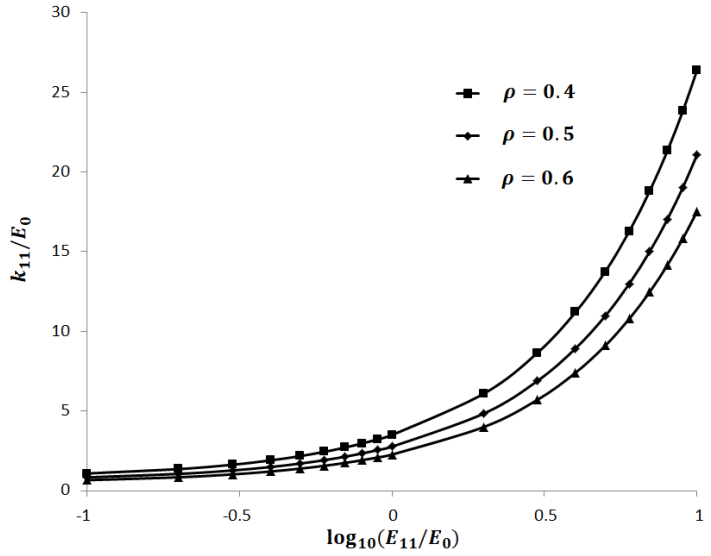

Figure 10. Plots of k_{11}/E_0, against $\log_{10}(E_{11}/E_0)$ for $E_{12}/E_0 = E_{21}/E_0 = E_{22}/E_0 = 1$ and $\rho = 0.4$, 0.5 and 0.6.

For $E_{12}/E_0 = E_{21}/E_0 = E_{22}/E_0 = 1$ and $\rho = 0.4$, 0.5 and 0.6, we plot k_{11}/E_0, k_{12}/E_0 and k_{22}/E_0 against $\log_{10}(E_{11}/E_0)$ in Figures 10, 11 and 12 respectively. Note that the values of k_{21} are observed to be very close to those of k_{12}. Figure 10 shows that the non-dimensionalized effective stiffness coefficient k_{11}/E_0 increases significantly as E_{11}/E_0 increases. For the values of E_{11}/E_0 smaller than 0.1, the magnitude of k_{11}/E_0 is extremely close to zero. From Figures 11 and 12, we find that k_{12}/E_0 and k_{22}/E_0 vary only very slightly with E_{11}/E_0 increases from 0.1 to 10. Thus, it appears that the micro-craze stiffness E_{11}/E_0 has a greater effect on k_{11}/E_0 than on k_{12}/E_0 and k_{22}/E_0.

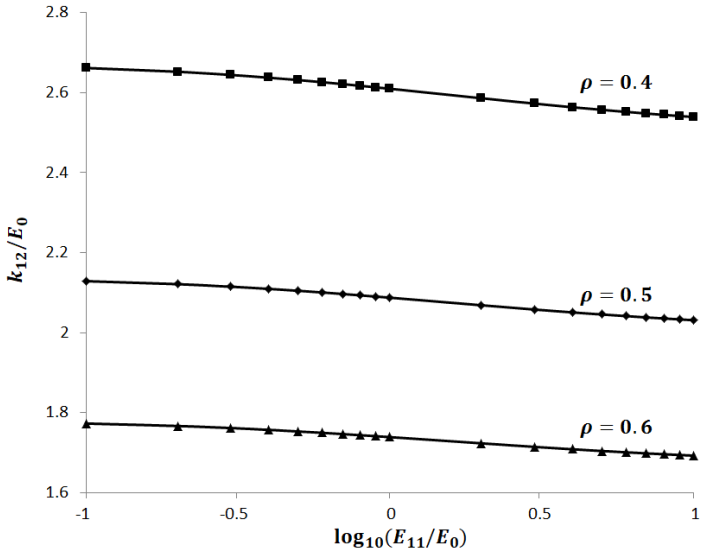

Figure 11. Plots of k_{12}/E_0, against $\log_{10}(E_{11}/E_0)$ for $E_{12}/E_0 = E_{21}/E_0 = E_{22}/E_0 = 1$ and $\rho = 0.4$, 0.5 and 0.6.

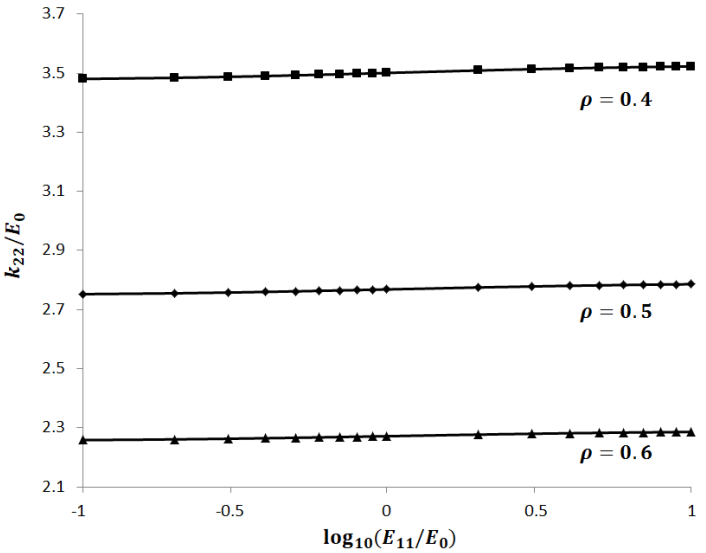

Figure 12. Plots of k_{22}/E_0, against $\log_{10}(E_{11}/E_0)$ for $E_{12}/E_0 = E_{21}/E_0 = E_{22}/E_0 = 1$ and $\rho = 0.4$, 0.5 and 0.6.

7 Summary

The current paper employs a micro-crazed interface model to estimate the effective stiffness k_{ij} of a soft imperfect interface between two dissimilar elastic half-spaces. The interface is modeled as a periodic array of identical micro-crazes. The micro-crazes contain main fibrils and cross-tie fibrils. The fibrils are modeled as a continuous distribution of anisotropic springs with stiffness E_{ij}.

The boundary conditions on the micro-crazes are formulated in terms of a system of hypersingular integro-differential equations where the unknown functions are directly the displacement jumps across the micro-crazes. Once the displacement jumps are obtained, the effective stiffness k_{ij} of the micro-crazed interface can be readily computed.

To investigate the effects of the micro-crazes on the effective stiffness of the micro-crazed interface, we take the materials in the half-spaces to be particular isotropic glassy polymers.

For case studies involving micro-crazes with only the main fibrils linking opposite micro-craze faces, we find that the only non-zero micro-craze stiffness given by E_{22} influences the effective stiffness k_{22} of the micro-crazed interface. There is negligible change in the other effective stiffness k_{12}, k_{21} and k_{11} when we vary E_{22} over a sufficiently wide range of value. As expected, k_{22} increases as E_{22} increases. For the case in which the micro-crazes are partially cracked, k_{22} decreases if the cracked parts of the micro-crazes become larger.

We also consider micro-crazes with both main and cross-tie fibrils to investigate the effects of varying E_{ij} on k_{ij}.The numerical calculations of k_{ij} show that E_{11}, E_{12} and E_{22} only have significant effects on the effective stiffness coefficients k_{11}, k_{12} and k_{22} respectively. (Note that $E_{21}(x)$ is chosen to

be equal to E_{12} and the computed values of k_{21} are found to be very close very close to those of k_{12}.)

In general, increasing the micro-craze density ρ decreases k_{ij}. For the case where E_{ij} are constants, we find that k_{ij} approaches E_{ij}as ρ approaches 1.

The micromechanical model proposed in the current paper has been successfully employed to gain useful physical insights into the effective behaviors of micro-crazed interfaces between glassy polymers. As far as we know, this is the first time a micro-crazed interface model has been used to estimate the effective behavior of a soft imperfect interface. From a practical standpoint, the results obtained are potentially useful as glassy polymers are widely used in engineering applications and the formations of micro-crazes have been observed on the interfaces between glassy polymers during manufacturing processes.

References

[1] Ang, W. T. *Hypersingular Integral Equations in Fracture Analysis,* Woodhead Publishing, Cambridge, 18-66 (2013).

[2] Benveniste, Y., and Miloh, T. Imperfect soft and stiff interfaces in two-dimensional elasticity. *Mechanics of Materials,* **33**(6), 309-323 (2001). https://doi.org/10.1016/S0167-6636(01)00055-2

[3] Brown, H. R. A molecular interpretation of the toughness of glassy polymers, *Macromolecules,* **24**(10), 2752-2756 (1991). https://doi.org/10.1021/ma00010a018

[4] Clements, D. L. *Boundary Value Problems Governed by Second Order Elliptic Systems*, Pitman, London, 30-120 (1981).

[5] Fan, H., and Keer, L. M. Two-dimensional line defects in anisotropic elastic solids, *International Journal of Fracture,* **62**(1), 25-42 (1993). https://link.springer.com/article/10.1007/BF00032523

[6] Fan, H., and Wang, G. F. Screw dislocation interacting with imperfect interface, *Mechanics of Materials,* **35**(10), 943-953 (2003). https://doi.org/10.1016/S0167-6636(02)00309-5

[7] Gent, A. N., and Thomas, A. G. Effect of molecular weight on the tensile strength of glassy plastics, *Journal of Polymer Science: Part A-2 Polymer Physics,* **10**(3), 571–573 (1972). https://doi.org/10.1002/pol.1972.160100314

[8] Hashin, Z. The spherical inclusion with imperfect interface, *ASME Journal of Applied Mechanics,* **58**(2), 444-449 (1991). https://doi:10.1115/1.2897205

[9] Hui, C. Y., Ruina, A, Creton, C., and Kramer, E. J. Micromechanics of crack growth into a haze in a polymer glass, *Macromolecules*, **25**(15), 3948-3955 (1992). https://doi.org/10.1021/ma00041a018

[10] Jones, J. P., and Whittier, J. S. Waves at a flexibly bonded interface, *Journal of Applied Mechanics,* **34**(4), 905-909 (1967). https://doi:10.1115/1.3607854

[11] Kaya, A. C., and Erdogan, F. On the solution of integral equations with strongly singular kernels, *The Quarterly of Applied Mathematics,* **45**(1), 105–122 (1987). https://doi.org/10.1090/qam/885173

[12] Kuo, C. C., Phoenix, S. L., and Kramer, E. J., Geometrically necessary entanglement loss during crazing of polymers, *Journal of Materials Science Letters,* **4**(4), 459–462 (1985). https://link.springer.com/article/10.1007%2FBF00719745?LI=true

[13] Sha, Y., Hui, C. Y., Ruina, A, and Kramer, E. J. Continuum and discrete modeling of crack failure at a crack tip in a glassy polymer, *Macromolecules*, **28**(7), 2450-2459 (1995). https://doi.org/10.1021/ma00111a044

[14] Sudak, L. J. On the interaction between a dislocation and a circular inhomogeneity with imperfect interface in antiplane shear, *Mechanics Research Communications,* **30**(1), 53-59 (2003). https://doi.org/10.1016/S0093-6413(02)00352-X

[15] Sudak, L. J. and Wang, X. Green's function in plane anisotropic bimaterials with imperfect interface, *IMA Journal of Applied Mathematics,* **71**(5), 783-794 (2006). https://doi.org/10.1093/imamat/hxl010

[16] Walton, J. R., and Weitsman, Y. Deformations and stress intensities due to a craze in an extended elastic material, *ASME Journal of Applied Mechanics,* **51**(1), 84-92 (1984). https://doi.org/10.1115/1.3167602

[17] Wang, W. V., and Kramer, E. J. A distributed dislocation stress analysis for crazes and plastic zones at crack tips, *Journal of Materials Science,* **17**(7), 2013–2026 (1982). https://link.springer.com/article/10.1007/BF00540419

[18] Wang, X., Ang, W. T., and Fan, H. Hypersingular integral and integrodifferential micromechanical models for an imperfect interface between a thin orthotropic layer and an orthotropic half-space under inplane elastostatic deformations, *Engineering Analysis with Boundary Elements,* **52,** 32-43 (2015). https://doi.org/10.1016/j.enganabound.2014.11.003

[19] Weitsman, Y. Nonlinear analysis of crazes, *Journal of applied mechanics,* **53**(1), 97-102 (1986). https://doi.org/10.1115/1.3171745

[20] Xiao, F., and Curtin, W. A. Numerical investigation of polymer craze growth and fracture, *Macromolecules,* **28**(5), 1654-1660 (1995). https://doi.org/10.1021/ma00109a043

[21] Xiao, Z. M., and Guo, J. Y. Deformation and stress Intensities of an interfacial craze with nonlinear fibrils, *International Journal of Nonlinear Sciences and Numerical Simulation,* **1**(4), 267-274 (2000). https://doi.org/10.1515/IJNSNS.2000.1.4.267

[22] Xiao, Z. M., and Pae, K. D. Stress analysis around a three-dimensional craze in glassy polymers, *Polymer Engineering and Science,* **33**(18), 1189-1194 (1993). https://doi.org/10.1002/pen.760331806

[23] Yang, A. C. M., and Kramer, E. J. Craze microstructure characterization by low-angle electron diffraction and Fourier transforms of craze images, *Journal of Materials Science,* **21**(10), 3601–3610 (1986). https://link.springer.com/article/10.1007/BF00553806

[24] Zhang, Y. M., Zhang, W. G., Fan, M., and Xiao, Z. M. On the interaction between a full craze and a near-by circular inclusion in glassy polymers, *Engineering Failure Analysis,* **79,** 441-454 (2017). https://doi.org/10.1016/j.engfailanal.2017.05.029

[25] Zhang, Y. M., Zhang, W. G., Fan, M., and Xiao, Z. M. Stress investigation on a cracked craze interacting with a near-by circular inclusion in polymer composites, *Acta Mechanica,* **228**(4), 1213-1228 (2017). https://link.springer.com/article/10.1007/s00707-016-1773-4